New design of distance protection for smart grid applications

Blumschein Jörg, Dzienis Cezary, Yelgin Yilmaz
Siemens AG, Energy Management Division, Berlín, Alemania

RESUMEN

Este artículo presenta un nuevo diseño de protección a distancia que se ajusta a los requerimientos futuros para las redes inteligentes, en lo que respecta a selectividad y confiabilidad. La medición de impedancia se basa en el cálculo de la reactancia de falla de carga compensada X y de la resistencia de línea separada de la resistencia de falla. Este método se aplica tanto a las fallas de fase a tierra como a las de fase a fase. La separación de la falla de resistencia mejora la precisión de los cálculos de impedancia. El método reduce la influencia negativa de la falla de resistencia durante el flujo alto de carga y minimiza el riesgo de hacer selecciones erróneas durante las condiciones de alta carga. Algunos criterios basados en magnitudes y cambios de los voltajes y corrientes, componentes simétricos o impedancias se aplican en paralelo. Los resultados de cada criterio individual se ponderan y se combinan para obtener el resultado final para la selección del lazo con falla. Con este principio de eficiencia, la selección del lazo ha sido optimizada para diferentes topologías de red mediante el cambio en la ponderación de cada criterio. Se aplica el mismo principio al elemento direccional.

PALABRAS CLAVE

Redes inteligentes de protección, relevo de protección.

ABSTRACT

This paper presents a new design of distance protection which perfectly fits to the requirements of the smart grid of the future, regarding selectivity and dependability. The impedance measurement is based on the calculation of the load compensated fault reactance X and from line resistance separated fault resistance. This method is applied for phase to ground as well as phase to phase faults. Separation of the fault resistance improves the accuracy of the impedance calculation. The method reduces the negative influence of fault resistance during high load flow and minimizes the risk of wrong pickup during high load condition. Several criteria based on magnitudes and changes of voltages and currents, symmetrical components or impedances are applied in parallel. The results of each single criterion are weighted and combined to get a final result for the selection of the faulted loop. With this principle the efficiency, the loop selection has been optimized to different network topologies by changing the weights of each criterion. The same principle is applied to the directional element.

KEY WORDS

Smart grid distance protection, protection relay.

Artículo publicado en el XII Simposio Iberoamericano sobre Protección de Sistemas Eléctricos de Potencia, 2015.

INTRODUCTION

Distance protection is used worldwide to protect the lines for the transmission and distribution of electrical energy against consequences of electrical faults. The distance protection has to detect these faults and initiate a trip command to isolate the faulted line.

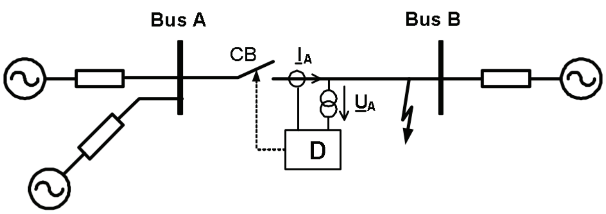

Fig. 1. Basic principle of distance protection.

These faults can be phase to phase which are short circuits between different phases or phase to ground which are short circuits between one or more phases and ground.

In most cases there will be an arc flash between the faulted phases or between phases and ground.

Figure 1 illustrates the basic principle of distance protection. The distance protection D determines the fault impedance Z_F from the voltage U_A and the current I_A measured at the relay location according to Ohm's law:

$$\underline{Z}_F = \frac{\underline{U}_A}{\underline{I}_A} \quad (1)$$

The measured fault impedance Z_F will be compared afterwards with the so called zone setting resulting from the line impedance. If the fault impedance is less than the configured setting the fault is on the line. In this case a trip command is issued to the local circuit breaker CB to isolate the faulted line from system operation as shown in figure 1.

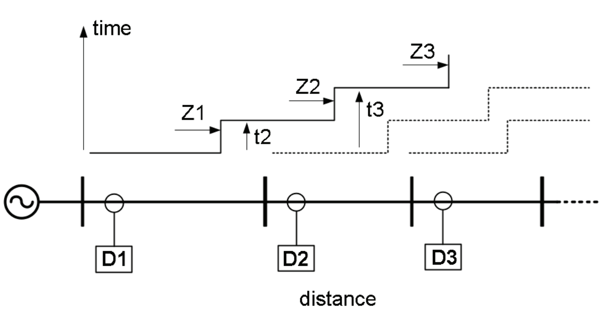

Fig. 2. Principle of stepped distance protection.

Figure 2 shows the principle of a stepped distance protection. For the selectivity it is important that only the faulted line is separated from operating network. That means that the relay D1 in 2 should only issue a non-delayed trip command if the fault is inside the protected zone Z1. Due to some uncertainty of the network parameters as well as measurement errors, this zone is normally configured to 80% of the protected line. Faults on adjacent lines should be tripped by the related relays D2 or D3 in 2. The relay D1 works only as a backup function for faults on these lines.

Most faults on transmission and distribution lines are not pure metallic faults but faults with a so called fault resistance like shown in 3. This fault resistance can be an arc flash for phase to phase faults or the combination of an arc flash and the grounding resistance for phase to ground faults.

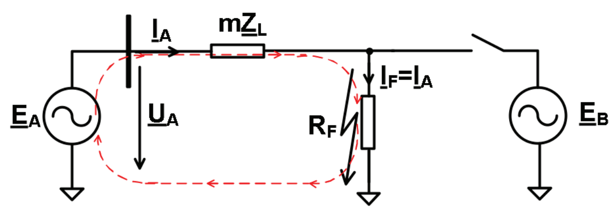

Fig. 3. Single phase diagram for a resistive fault.

In reality the model of an arc flash is much more complicated but for simplicity it will be modeled as a fault resistance R_F in this paper.

In case of faults including resistance R_F, the equation for the faulted loop can be obtained based on 3 as follows:

$$\underline{U}_A = (m \cdot \underline{Z}_L + R_F) \cdot \underline{I}_A \quad (2)$$

According to (2), the impedance measured by the distance protection consists of two parts. The first part $m*\underline{Z}_L$ is the impedance of the line between the relay and the point of the fault. The second part R_F is the fault resistance, representing the resistance of the arc flash for phase to phase faults or the combination of an arc flash and the grounding resistance for phase to grounding resistance for phase to ground faults.

Figure 4 shows the graphical representation of both impedances in the complex plane. The phasor of $m*\underline{Z}_L$ is shown at the line angle which is close to 90° for high voltage overhead lines. The phasor representing fault resistance R_F is added in parallel to the R-axis.

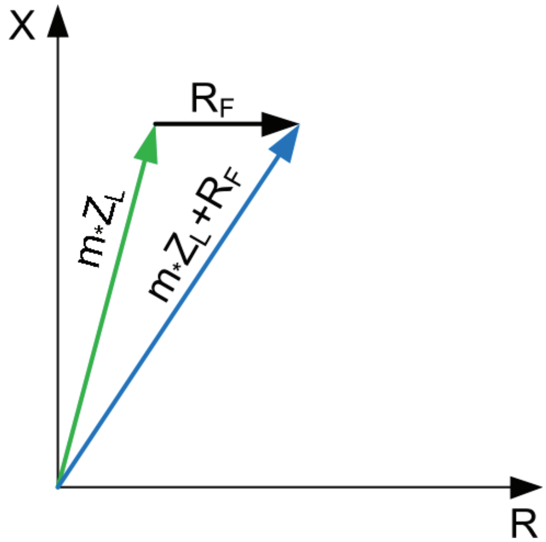

Fig. 4. Graphical representation resistive fault in the complex plane.

Depending on the fault position m the fault impedance m*$\underline{Z}_L$ can vary between zero for faults close to the relay and 0.8*$\underline{Z}_L$ for faults at the end of the protected zone. The polygonal characteristic is the best choice because this characteristic has a constant reach in R-direction for all faults on the protected line.

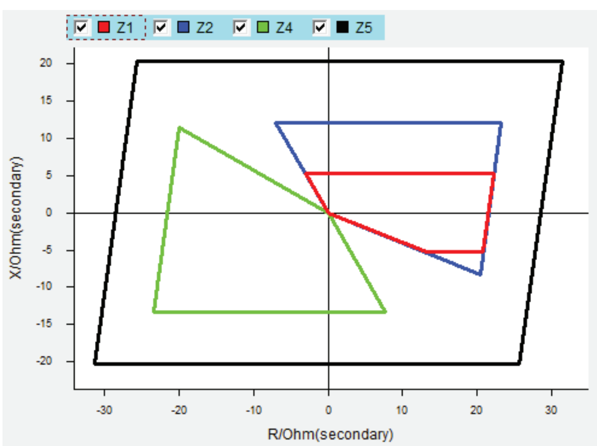

Fig. 5. Typical polygonal characteristic of a stepped distance protection.

Figure 5 represents a typical polygonal characteristic of a stepped distance protection. According to the principle explained in 2 the red marked zone Z1 is responsible to detect faults up to 80% of the protected line. In this case a non-delayed trip command is issued. The blue marked zone Z2 has the same reach in R-direction but can detect faults up to 150% of the protected line. Normally zone Z2 is delayed by 300 ms to have a backup function. The green marked zone Z4 is a backup zone for the reverse direction and the black marked zone Z5 is another unidirectional backup zone.

The distance protection has the great advantage of selectivity which can be achieved by local measurement only without any communication.

IMPEDANCE MEASUREMENT ON HEAVY LOADED LINES

The classical impedance measurement according to (2) is only accurate for lines with single ended infeed as well as without significant load.

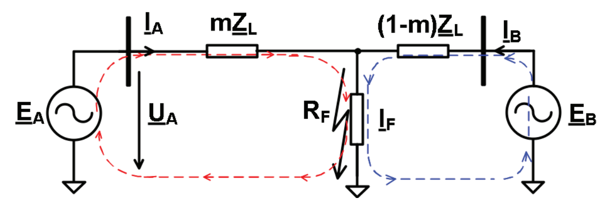

Fig. 6. Single line diagram for a resistive fault, feeded from both ends of the line.

Figure 6 shows the single line diagram for a resistive fault, feeded from both ends of the line. In this case the fault current I_F is the sum of the fault current I_A from the local end and the fault current I_B from the remote end.

The local relay at bus A can only measure the current I_A from the local end. But with regard to 6 the fault current from the remote end causes an additional voltage drop at the fault resistance R_F

$$\underline{U}_A = (m \cdot \underline{Z}_L + R_F) \cdot \underline{I}_A + R_F \cdot \underline{I}_B \quad (3)$$

This additional voltage drop caused by the fault current from the remote end has an impact on the accuracy of impedance measured by the distance protection at bus A. This voltage drop results in an additional impedance component which depends on the relation between the local fault current I_A and the fault current $\underline{I}_B$ from the remote end.

$$\underline{Z}_A = (m \cdot \underline{Z}_L + R_F) + \frac{\underline{I}_B}{\underline{I}_A} R_F \quad (4)$$

According to (4) this additional impedance is increasing with increasing fault current contribution from the remote end. The additional impedance can have a reactive component if the fault currents I_A and $\underline{I}_B$ have different angles. This reactive component will result in a measuring error ΔX if the classical impedance measuring method (2) is applied in distance protection:

$$\Delta X = \frac{|\underline{I}_B|}{|\underline{I}_A|} \cdot R_F \cdot \sin\left(\angle(\underline{I}_B, \underline{I}_A)\right) \qquad (5)$$

Transmission of active power requires a phase difference between the voltages of the equivalent sources at sending and receiving end. During load flow the phase angle of the sending end leads the phase angle of the receiving end. In case of a fault the phase angles of the fault current contributions from both ends are related to the phase angles of the feeding voltages in a first approach.

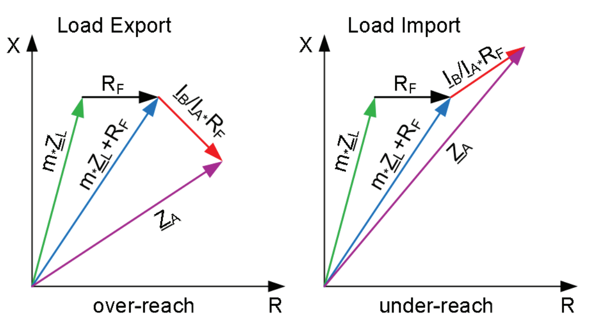

Fig. 7. Influence of the remote end infeed on the impedance calculation of a resistive fault using the classical impedance calculation method.

Figure 7 illustrates the influence of the load flow on the calculated impedance of a resistive fault using the classical impedance calculation method. In case of load export the phase angle of I_A leads the phase angle of I_B. According to (5), ΔX becomes negative for a normal load angle of 30° which results in an overreach of the distance protection.

A simulated case from the network of Colombia is used to explain the opposite case. A fault AB-N with 5 Ω fault resistance is applied at 50% line length of a heavy loaded line. This case was tested with a distance protection relay using the classical impedance calculation method.

Referring to 8 there is a load import of 122 MW before the fault occurred. At fault inception the load flow is changing the direction to feed the fault from the local source. The binary signals indicate that this fault was not seen in zone Z1 even if the fault was applied at 50% of the line length, whereas the reach of zone Z1 was configured to 80% of the line length. A trip command was issued by the overreach zone Z1B supported by the receive signal from teleprotection. 9 illustrates the measured impedance in the complex plane. The fault was applied at 50% of the line length but according to the principle explained in 7 the measured impedance is located outside the red marked zone Z1 which is configured to 80% of the line length.

According to (5) the phenomenon of overreach or underreach for resistive faults only effects heavy loaded lines with infeed from both ends. In the past this effect was compensated by changes to the characteristic of the zones.

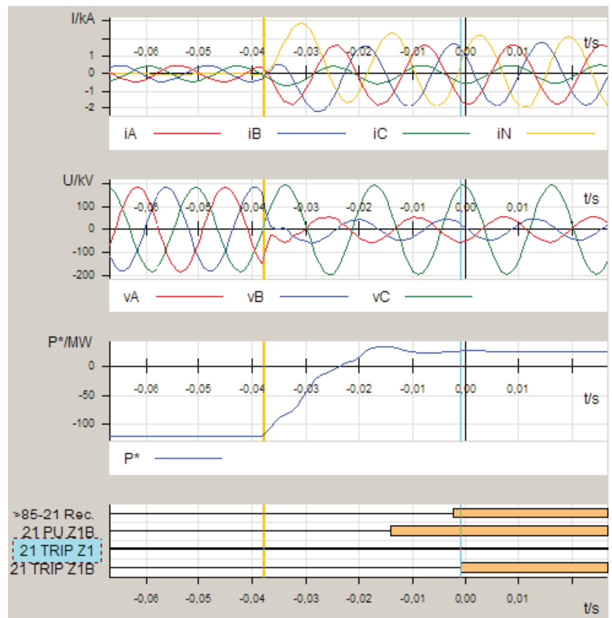

Fig. 8. Fault record of a resistive fault at 50% of the line length which is not seen in Z1 using the classical impedance calculation method.

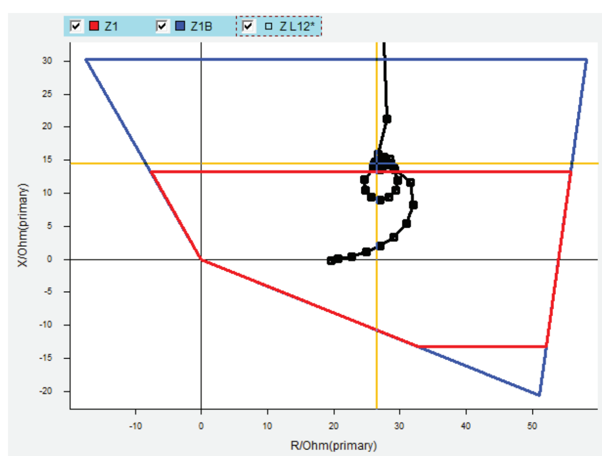

Fig. 9. Impedance plane of a resistive fault at 50% of the line length which is not seen in Z1 using the classical impedance calculation method.

Today and in the smart grids of the future such a static compensation is not sufficient because the load often changes in magnitude or direction.

IMPEDANCE MEASUREMENT WITH LOAD COMPENSATION

The general idea of the impedance measurement with load compensation is the elimination of the reactance measurement error ΔX given in (5).

According to 6, ec. (3) can be written in the following form:

$$\underline{U}_A = m \cdot \underline{Z}_L \cdot \underline{I}_A + R_F \cdot \underline{I}_F \tag{6}$$

To eliminate the reactance measurement error ΔX caused by the fault resistance R_F multiplied with the complex fault current I_F, eq. (6) will be multiplied with a compensation quantity which is the conjugate-complex value of the fault current I_F. This compensation quantity consists a compensation current I_{Cmp} which should be already very closed to I_F and a compensation angle δ_{Cmp} for the final adjustment

$$\underline{U}_A \cdot \underline{I}^*_{Cmp} \cdot e^{-j\delta_{Cmp}} = m \cdot \underline{Z}_L \cdot \underline{I}_A \cdot \underline{I}^*_{Cmp} \cdot e^{-j\delta_{Cmp}} + R_F \cdot \underline{I}_F \cdot \underline{I}^*_{Cmp} \cdot e^{-j\delta_{Cmp}} \tag{7}$$

Due to the multiplication of I_F with its conjugate-complex replacement the term $R_F{*}I_F{*}\ I^*_{Cmp}{*}e^{-j\delta Cmp}$ becomes a real value. For the calculation of the fault reactance only the imaginary part of (7) needs to be considered

$$\mathrm{Im}\left[\underline{U}_A \cdot \underline{I}^*_{Cmp} \cdot e^{-j\delta_{Cmp}}\right] = \mathrm{Im}\left[m \cdot \underline{Z}_L \cdot \underline{I}_A \cdot \underline{I}^*_{Cmp} \cdot e^{-j\delta_{Cmp}}\right] \tag{8}$$

Solving for X, which is the imaginary part of $m{*}Z_L$, we get

$$X = \frac{\sin(\varphi) \cdot \mathrm{Im}[\underline{U}_A \cdot \underline{I}^*_{Cmp} \cdot e^{-j\delta_{Cmp}}]}{\mathrm{Im}[e^{j\varphi} \cdot \underline{I}_A \cdot \underline{I}^*_{Cmp} \cdot e^{-j\delta_{Cmp}}]} \tag{9}$$

It is shown, that the zero sequence current I_0 or the negative sequence current I_2 can be used as a compensation current for the fault current I_F because they are not influenced by load flow.

In case of different impedance angles in the zero or negative sequence network a final adjustment can be done using as example for the zero sequence.

$$\delta_{Cmp,0} = \arg\left\{\frac{\underline{Z}_{0,A} + \underline{Z}_{0,B} + \underline{Z}_{0,L}}{(1-m) \cdot \underline{Z}_{0,L} + \underline{Z}_{0,B}}\right\} \tag{10}$$

Using this compensation angle $\delta_{Cmp,0}$ the measured zero sequence current $I_{0,A}$ can be adjusted to the angle of the fault current I_F if the zero sequence impedances $Z_{0,A}$, $Z_{0,B}$ and $Z_{0,L}$ have different angles.

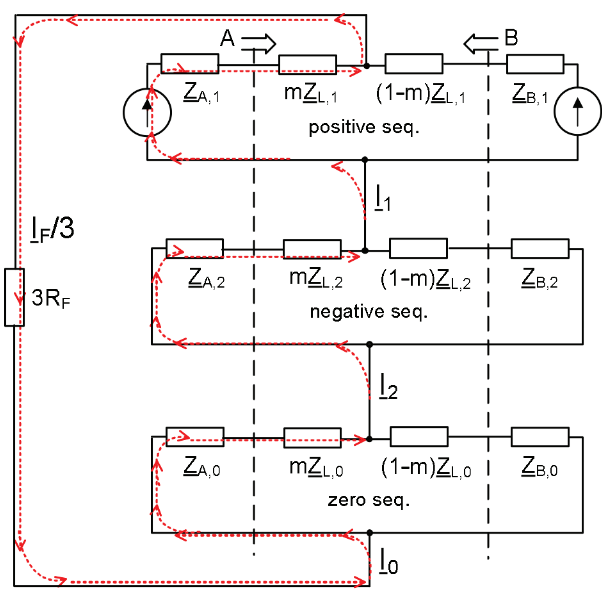

Fig. 10. Sequence network for a single phase to ground fault.

IMPEDANCE MEASUREMENT FOR PHASE TO PHASE LOOPS USING REACTANCE METHOD

The basic idea to compensate the influence of load flow can be extended to phase to phase faults. 11

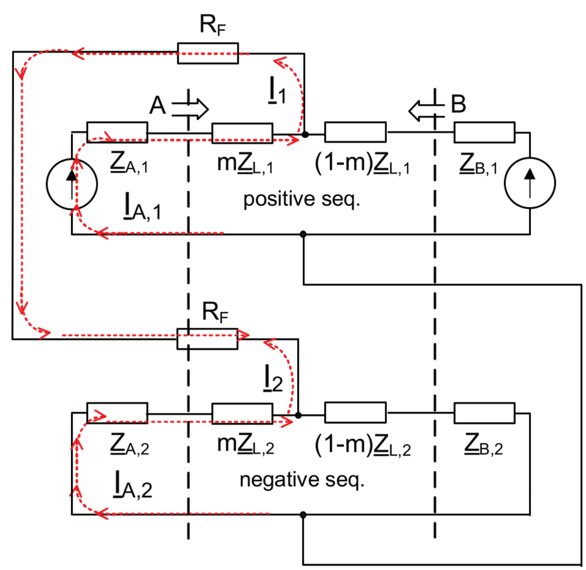

Fig. 11. Sequence network for a phase to phase fault.

shows the current flow for a phase to phase fault with the fault resistance R_F in the sequence network.

For a phase to phase fault the negative sequence network is connected in parallel to the positive sequence network. Since the zero sequence component does not exist for a phase to phase fault and the positive sequence network includes the sources only the negative sequence current can be used as compensation quantity.

The determination of the compensation quantity for phase to phase faults will be explained using an AB fault as example. For an AB fault the fault current I_F is the difference between the current of phase A and the current of phase B

$$\underline{I}_F = \underline{I}_A - \underline{I}_B \tag{11}$$

Replacing the phase currents by the sequence components we get the following result:

$$\begin{aligned} \underline{I}_A &= \underline{I}_1 + \underline{I}_2 \\ \underline{I}_B &= \underline{a}^2 \cdot \underline{I}_1 + \underline{a} \cdot \underline{I}_2 \end{aligned} \tag{12}$$

For the AB fault the relation between positive sequence current and negative sequence current is given as:

$$\underline{a} \cdot \underline{I}_1 = -\underline{a}^2 \cdot \underline{I}_2 \tag{13}$$

Considering this transformation factor the compensation current for the AB fault based on the negative sequence current can be derived:

$$\underline{I}_{Cmp,AB} = 2 \cdot (1-\underline{a}) \cdot \underline{I}_2 \tag{14}$$

For other fault types the compensation quantity will be determined accordingly. In case of different impedance angles in the negative sequence network a final adjustment can be done using

$$\delta_{Cmp,2} = \arg\left\{ \frac{\underline{Z}_{2,A} + \underline{Z}_{2,B} + \underline{Z}_{2,L}}{(1-m) \cdot \underline{Z}_{2,L} + \underline{Z}_{2,B}} \right\} \tag{15}$$

The exact reactance for a resistive fault AB on heavy loaded lines can be calculated using the following equation.

$$X = \frac{\sin(\varphi) \cdot \mathrm{Im}[\underline{U}_{AB} \cdot (\underline{I}_{Cmp,AB} \cdot e^{j\delta_{Cmp,2}})^*]}{\mathrm{Im}[e^{j\varphi} \cdot (\underline{I}_A - \underline{I}_B) \cdot (\underline{I}_{Cmp,AB} \cdot e^{j\delta_{Cmp,2}})^*]} \tag{16}$$

This method was applied to the fault explained in section 2. As shown in 12 the fault is seen in zone Z1 using the impedance calculation based on the reactance method.

Consequently with the new method of reactance compensation for resistive faults on heavy loaded lines a trip command in zone Z1 for the fault simulated for a network in Colombia is issued as shown in 13.

According to[1] the method of reactance compensation can also be applied for 3 phase fault using the adequate compensation quantity.

MULTICRITERIAL LOOP SELECTION

The proper selection of the faulted loops is a precondition for each distance protection algorithm. Different criteria are applied to select the faulted loops like:

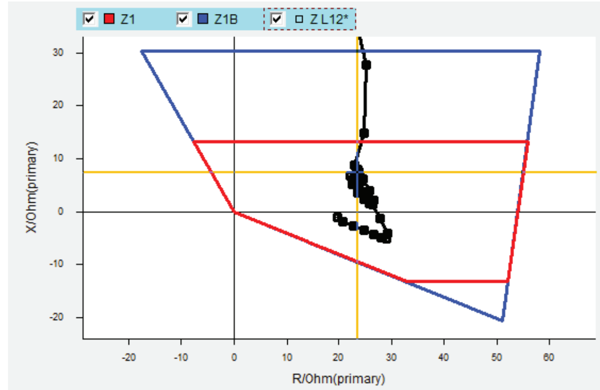

Fig. 12. Impedance plane for a resistive fault at 50% of the line length which is seen in Z1 using impedance calculation according to the reactance method.

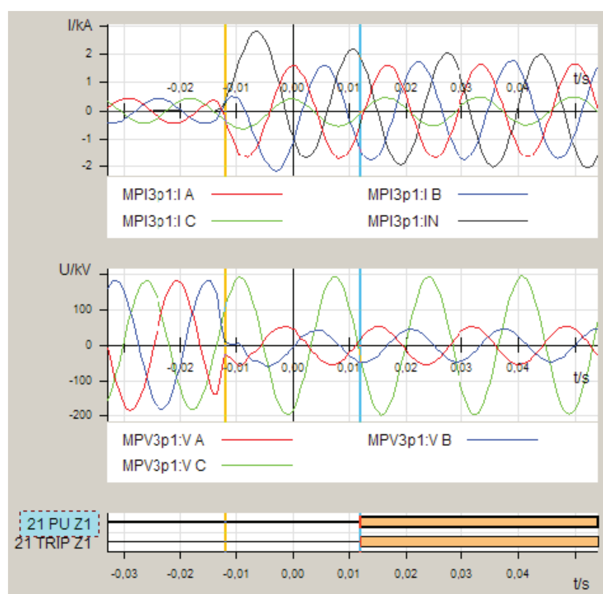

Fig. 13. Fault record of a resistive fault at 50% of the line length which is seen in Z1 using impedance calculation based on the reactance method.

- magnitude of currents and delta currents,
- magnitudes of voltages and delta voltages,
- impedances,
- symmetrical components.

In the past these different criteria were applied in form of a decision tree like illustrated in 14.

This decision tree was optimized to get the final result as fast as possible. Due to the structure of the decision tree not all criteria are evaluated to get a final result. From 14 it is obvious that a wrong loop can be determined if only one criterion gives a wrong result. Sometimes the result of a single criterion is not very strong but in the decision tree it must be reduced to binary information. Additional to this it was shown by simulations and analysis of real events that different criteria have different importance for different network topologies.

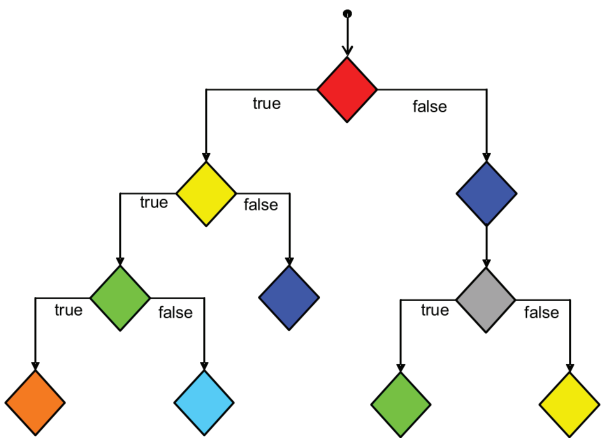

Fig. 14. Decision tree as classical structure for the loop selection.

All these considerations lead to another structure of the loop selection like shown in 15.

With the new concept all criteria of loop selection are applied in parallel creating the so called multi-criteria loop selector. Each criterion can have an output quality which is a value between 0.0 ---which means the criterion is not fulfilled--- and 1.0 ---which means the criterion is completely fulfilled.

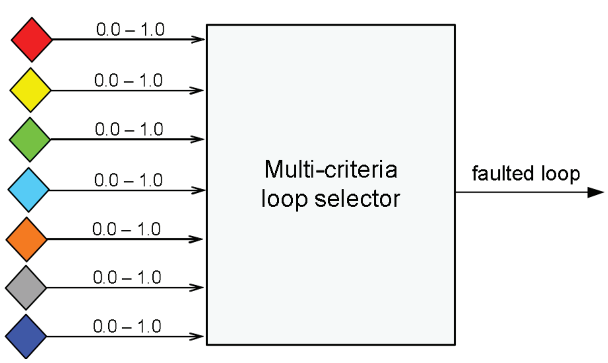

Fig. 15. Multi-criteria loop selection.

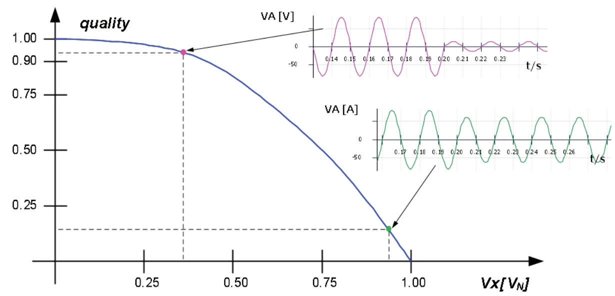

Fig. 16. Quality of criteria voltage.

Figure 16 gives an example of the output quality of the voltage criterion. A strong voltage drop in case of a fault results in a high quality of the voltage criterion for the related loop. If the voltage drop is only marginal the quality of the voltage criteria of the related loop will have a low quality.

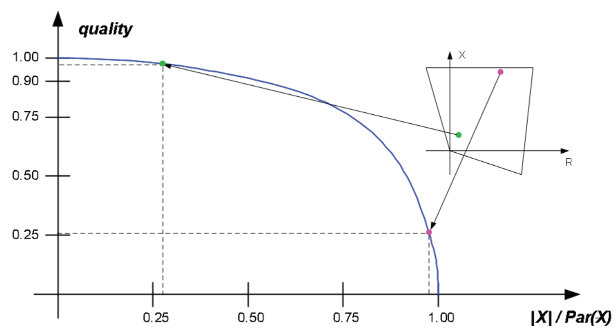

Fig. 17. Quality of criteria impedance.

Figure 17 illustrates the output quality of the impedance criterion. If the measured loop impedance is closed to the zone limit the quality of the impedance criteria is low. However if it is clear that the impedance is in the zone the related quality is high.

According to equation (17) a final quality Q_{loop} for each loop will be calculated. The weighted quality outputs of N criteria $q_{i,loop}$ will be summated to get the final quality Q_{loop}.

$$Q_{loop} = \sum_{i=1}^{N} q_{i,loop} \cdot x_i \qquad (17)$$

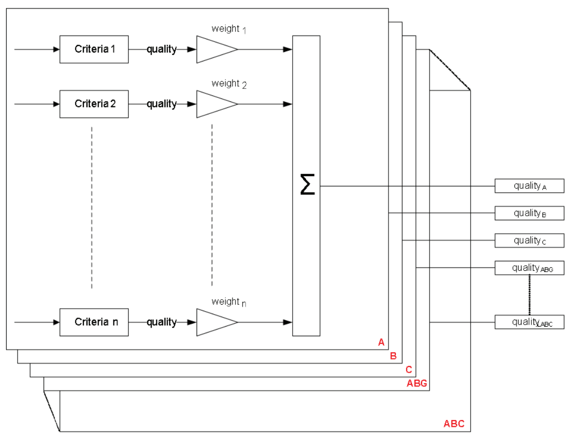

Fig. 18. Calculation of loop quality.

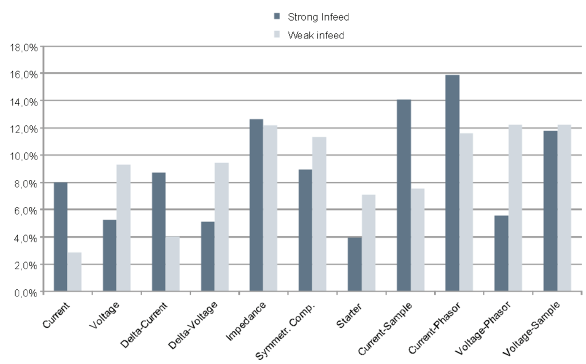

Fig. 19. Weights of multi-criteria loop selector depending on different infeed.

Figure 18 gives a graphical explanation of equation (17). It is shown that each criterion is weighted according to its significance.

It was found by simulations and analysis of real events that depending on network topologies different criteria have different significance.

Figure 19 gives an example for the best adaption of the weights for a network with strong infeed compared to a network with weak infeed. It is obvious that the current based criteria have a higher weight in a network with strong infeed however the voltage based criteria have a higher weight in networks with weak infeed. By implementing the

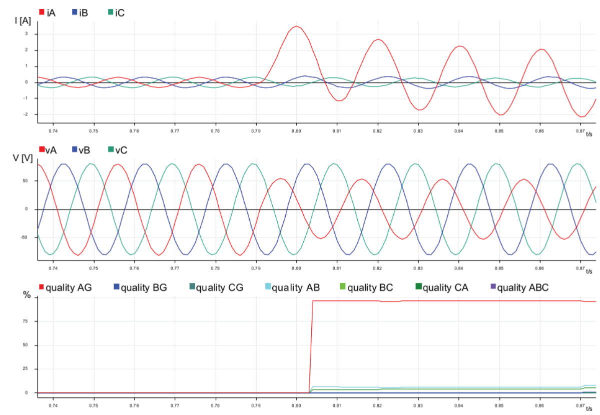

Fig. 20. Operation of the multi-criteria loop selector.

weighting factors between the boundaries shown in 19 the loop selection is optimized for all system conditions.

Figure 20 illustrates the operating principle of the multi-criteria loop selector. After fault inception the qualities for all loops are calculated. A loop is selected if the quality of the loop extends an adaptive threshold like shown in figure 20.

CONCLUSION

It was shown that the reach of the classical impedance calculation method is significantly influenced by resistive faults on heavy loaded lines. Using the reactance method this reach error can be eliminated. Additionally a new method of loop selection was presented which is optimized for all network topologies. The same philosophy is applied for directional element where different algorithm are weighted and depended on network topology.

BIBLIOGRAFÍA

C. Dzienis, Y. Yelgin, G. Steynberg, et al., Novel impedance determination method for phase-to-phase loops, 18th Power Systems Computation Conf., Aug. 2014.